Simultaneous Estimation of Poisson's Ratio and Young's Modulus using a Single Indentation: A Finite Element Study

Zheng YP[1, 2], Choi APC[1], Ling HY[1], and Huang YP[1]

[1] Department of Health Technology and Informatics, [2] Research Institute of Innovative Products and Technologies, The Hong Kong Polytechnic University

Hung Hom, Kowloon, Hong Kong

Running Title: **Estimation of Poisson's Ratio from Indentation**

Corresponding author:

Dr. Yongping Zheng

Department of Health Technology and Informatics,

The Hong Kong Polytechnic University,

Hung Hom, Kowloon, Hong Kong SAR, P.R.China

Tel: 852-27667664

Fax: 852-23624365

E-mail: ypzheng@ieee.org

Submitted to: Measurement Science and Technology

Submitted on: Nov 19 2008

Abstract --- Indentation is commonly used to determine the mechanical properties of different kinds of biological tissues and engineering materials. With the force-deformation data obtained from an indentation test, the Young's modulus of the tissue can be calculated using a linear elastic indentation model with a known Poisson's ratio. A novel method for simultaneous estimation of the Young's modulus and the Poisson's ratio of the tissue using a single indentation was proposed in this study. Finite element (FE) analysis using 3D models was first used to establish the relationship between the Poisson's ratio and the deformation-dependent indentation stiffness for different aspect ratios (indentor radius/ tissue original thickness) in the indentation test. From the FE results, it was found that the deformation-dependent indentation stiffness linearly increased with the deformation. The Poisson's ratio could be extracted based on the deformation-dependent indentation stiffness obtained from the force-deformation data. The Young's modulus was then further calculated with the estimated Poisson's ratio. The feasibility of this method was demonstrated in virtue of using the indentation models with different material properties in the FE analysis. The numerical results showed that the percentage errors of the estimated Poisson's ratios and the corresponding Young's moduli ranged from -1.7% to -3.2% and 3.0% to 7.2%, respectively, with the aspect ratio (indentor radius / tissue thickness) larger than 1. It is expected that this novel method can be potentially used for quantitative assessment of various kinds of engineering materials and biological tissues, such as articular cartilage.

Keywords: indentation; Young's modulus; Poisson's ratio; finite element analysis; ultrasound indentation; nano-indentation; articular cartilage; soft tissues

1. INTRODUCTION

Indentation has been commonly used to study the mechanical properties of different kinds of engineering materials and biological soft tissues in the past decades [1,2]. A typical example is for the assessment of articular cartilage. The indentation on articular cartilage can be performed *in-vitro* [3-7], or *in-vivo* via arthroscopy [8-10]. Hayes et. al. (1972) reported a rigorous mathematical solution for the indentation of a thin elastic layer bonded on a rigid half-space which is similar to the cartilage-bone structure [11]. The tissue was assumed to be linear elastic, homogenous and isotropic and only an infinitesimal deformation was considered. The Young's modulus of tissue can be obtained by the following equation using a flat ended cylindrical indentor:

$$E = \frac{(1-v^2)}{2a\kappa(v, a/h)} \cdot \frac{P}{w} \qquad (1)$$

where E is Young's modulus, P is indentation force, v is Poisson's ratio, w is deformation, a is indentor radius, h is tissue thickness, and κ is a scaling factor, which depends on different aspect ratios *a/h* and Poisson's ratios *v*. In their study, they calculated the value of κ using numerical solution for $0.3 \le v \le 0.5$. Jurvelin (1991) further estimated the values of κ for which v is smaller than 0.3 [12]. Zhang et. al. (1997) reported a new table of κ by using nonlinear finite element (FE) analysis to include the effects of finite deformations [13]. It was found that κ increased almost linearly with the indentation depth, i.e. tissue deformation. Their result obtained under the infinitesimal deformation was comparable with that reported by Hayes.

Both indentor radius a and tissue thickness h can be obtained in advance before an indentation test, in which h can be measured directly or evaluated from needle punch [14], optical or ultrasound methods [15,16] for articular cartilage. The instantaneous Poisson's ratio was generally assumed to be a constant value varied from 0.45-0.5 in previous studies [1] for soft tissues. κ can be estimated based on the table reported by Hayes or Zhang. During the indentation test, both indentation force P and tissue deformation w in Eq. (1) can be determined with various methods. P can be obtained from strain gauges [16] and fiber optic sensor [17], while w can be measured by a displacement transducer, such as linearly variable differential transformer (LVDT) [18], spatial sensors [19] or ultrasonic methods [8,9,16,20]. Consequently, the Young's modulus E can be evaluated by using Eq. (1) associated with the force-deformation data obtained from the indentation. However, the estimation error of Young's modulus may be greatly increased due to the incorrect assumption of the Poisson's ratio in Eq. (1).

The Poisson's ratio of articular cartilage has been measured by optical and mechanical methods [21]. In the optical measurements, an axial load was applied and the strain in the lateral direction was then measured using microscope in order to calculate the Poisson's ratio. On the other hand, confined and unconfined compressions were conducted by the mechanical method to determine the aggregate modulus H_a and Young's modulus E, respectively. The Poisson's ratio was calculated using the following equation,

$$H_a = \frac{1-\nu}{(1+\nu)(1-2\nu)} \cdot E \, . \qquad (2)$$

These two methods can be used to determine the corresponding Poisson's ratio of the tissues effectively. However, both methods can only work *in-vitro* but not *in-vivo*, as the soft tissue has to be excised. A number of studies have been reported to use ultrasound elastography, i.e. imaging tissue strains using ultrasound, to estimate Poisson's ratio [22-25]. The basic principle is to use ultrasound imaging to obtain the strains of a local tissue in two directions of the imaging plane under a static loading. To achieve the *in-vivo* measurement, Jin and Lewis (2004) reported a new approach to calculate the Poisson's ratio via two indentation tests with two different sized indentors [26]. The Poisson's ratio is obtained by

$$\frac{P_1/w_1}{P_2/w_2} = \frac{a_1}{a_2} \cdot \frac{\kappa(a_1/h, v)}{\kappa(a_2/h, v)} \tag{3}$$

where the subscripts 1 and 2 represent the data related to the measurements using indentors 1 and 2, respectively. Since Eq.(4) was derived based on Eq. (1), Eq. (3) is only valid for the infinitesimal indentation. This method has been further improved by including the nonlinear effect of finite deformation [27]. The modified Eq. (3) which includes a deformation-dependent scaling factor κ_n is as follow,

$$\frac{P_1/w_1}{P_2/w_2} = \frac{a_1}{a_2} \frac{\kappa_n(a_1/h, v, w/h)}{\kappa_n(a_2/h, v, w/h)} . \tag{4}$$

Eq. (4) is similar to the Eq. (3), excepted that κ_n is deformation-dependent. With the consideration of the finite deformation, this method provides a new approach for simultaneous estimation of the Young's modulus and the Poisson's ratio in two indentation tests with two different sized indentors. However, the necessity of using two indentors may greatly reduce the flexibility of this method. In the field of nano-indentation for engineering material and coating measurement, a number of techniques have also been proposed to extract Poisson's ratio from indentation data. Lucas et al (2004) proposed a nano-indentor with multidimensional contact mechanics to measure Poisson's ratio [28]. During the indentation, the displacements and forces in three dimensions were measured. Jennett et al. (2003) reported to method to estimate Poisson's ratio by combining nano-indentation with surface acoustic wave measurement [29]. Huber and coworkers [30,31] proposed to use a single spherical indentation together with artificial neural networks to estimate Poisson's ratio of a thin layer of material. Ling et al. (2007) proposed a method to extract Poisson's ratio from cylindrical indentation data using genetic algorithms [32]. Although the use of neural networks and genetic algorithms, which requires training and parameter adjustment for different setups and are both time consuming, make the procedure be complicated, these studies demonstrated the feasibility of using the force-indentation data of a single indentation test to estimate Poisson's ratio.

In this study, we developed a new method for the simultaneous estimation of the Young's modulus and the Poisson's ratio using a single cylindrical indentation test alone and a simple calculation method. The relationship between the Poisson's ratio and the deformation-dependent indentation stiffness was established for different aspect ratios of indentor radius / tissue thickness. The algorithm of this method and preliminary validation using a finite element (FE) analysis were reported in this paper.

2. METHODS

According to the study of Zhang *et al*. [13], Hayes' indentation solution shown in Eq.(1) can be improved by taking into account the finite deformation effect as

$$E = \frac{\left(1-v^2\right)}{2a\kappa_n\left(a/h, v, w/h\right)} \cdot \frac{P}{w}. \quad (5)$$

In comparison with Eq. (1), κ_n in Eq. (5) depends on not only aspect ratio *a*/*h* and Poisson's ratio *v*, but also deformation ratio *w*/*h*. Moreover, it was revealed that κ_n linearly depends on the deformation *w,* and the correlation coefficients *r* are larger than 0.995, indicating a very good linearity. Therefore, κ_n can be written as

$$\kappa_n\left(a/h, v, w/h\right) = \kappa\left(a/h, v\right) \cdot \left(1+\beta\, w/h\right) \quad (6)$$

where β is a factor that depends on the Poisson's ratio and the aspect ratio between indentor radius and tissue thickness, i.e. $\beta = \beta\left(a/h, v\right)$. We extract different β data for the case of various *a*/*h* (0.2 ~ 2) and *v* (0.1 ~ 0.5) from the κ_n data obtained by Zhang *et al.* [13] to form a β table. This β table is then used to estimate the Poisson's ratio from the deformation-dependent indentation stiffness, *P/w*, which can be obtained from an indentation test. By substituting Eq. (6) into Eq. (5), the deformation-dependent indentation stiffness can be written as

$$P/w = c + c\beta \cdot w/h \quad (7)$$

where

$$c = \frac{2 \cdot a \cdot E}{\left(1 - v^2\right)} \kappa\left(a/h, v\right) \tag{8}$$

is the y-intercept of the linear relationship between P/w and w/h. The slope of this linear relationship is $c\beta$.

From an indentation test, we can obtain pairs of P and w, as well as the original tissue thickness h, using ultrasound techniques [9,16,20] or other methods. Therefore, y-intercept c and slope $c\beta$ in Eq. (7) can be easily calculated from the indentation data using a linear regression for P/w and w/h, then β can be obtained. Since the aspect ratio a/h is known for a specific indentation test, v is the only unknown. By the interpolation using β data and a/h from the β table, which was formed from the κ_n data [13], the Poisson's ratio v can be estimated. After obtaining the Poisson's ratio, we can use this Poisson's ratio v together with the y-intercept c, radius of indentor a, scaling factor $\kappa\left(a/h, v\right)$ and original thickness h to calculate the Young's modulus using Eq. (8).

In order to verify the feasibility of the proposed method, a commercial FE package (ABAQUS software, Version 6.2, Hibbitt, Karlsson & Sorensen, Inc, US) was employed to simulate indentation tests with various aspect ratio and Poisson's ratio. The simulated force-deformation data was then used to calculate the Young's modulus and Poisson's ratio, which were compared with the assigned Young's modulus and Poisson's ratio for the FE models. In this case, those assigned Young's modulus and Poisson's ratio were set to be 60 kPa and 0.45 respectively. In consistence with our previous ultrasound indentation test, the radius of the indentor was set to be 4.5 mm in the simulation [16]. Several FE models were built with different dimensions to simulate different aspect ratio *a*/*h* (0.6, 0.8, 1, 1.5 and 2). The deformation-dependent indentation stiffness was obtained from the FE analysis with various deformation ratio *w*/*h* (0.01, 0.025, 0.05 and 0.1), and used to estimate the Poisson's ratio and Young's modulus. In addition, different fixed Poisson's ratios (ν = 0.3 ~ 0.5) were used in the calculation of Young's modulus to show the estimation error in order to test the effect of incorrect estimation of Poisson's ratio in the estimation of Young's modulus.

3. RESULTS

The percentage difference between the scaling factors κ for the infinitesimal deformation obtained by the FE model in the current study, which was established based on the model used by Zhang *et al*. [13] for $0.1 \le \nu \le 0.5$, and those reported by Hayes *et al*. [11] for $0.3 \le \nu \le 0.5$ and Jurvelin [12] for $0.1 \le \nu \le 0.2$, is within ±3.5% (Table 1). The κ values increase with the increase of aspect ratios (0.2 ~ 2.0), Poisson's ratios (0.1 ~ 0.5) and deformation ratios (0 ~ 0.1) (Table 2). The results were obtained by linear interpolations of the data reported in Zhang *et al*. [13]. It was found that the κ increases linearly with the increase of the relative deformation ratio *w/h* [13], and the correlation coefficients *r* are larger than 0.995, indicating a very good linearity. The factor β monotonically increases as the increase of different Poisson's ratio (ν=0.1 ~ 0.5) for different aspect ratios (*a/h*=0.2 ~ 2.0) (Table 3). The nonlinear but monotonic relationships between the deformation-dependent indentation stiffness and the Poisson's ratio for different aspect ratio can be better illustrated using a figure (Fig. 1). For a specific value of β, there will be only one corresponding Poisson's ratio for a selected aspect ratio.

It was found that a quadratic function could fit the force-deformation data obtained from the indentations with different aspect ratios (*a/h*) and Poisson's ratios (v), with the correlation coefficient r close to 1 (Fig. 1). Fig. 2 shows the typical force - deformation curve, which is slightly nonlinear and can be fitted by a quadratic function. The corresponding relationship between the indentation stiffness (P/w) and the deformation ratio (w/h) could be represented using linear regressions for different deformation ratios including 1%, 2.5%, 5% and 10% (for the case with a/h= 2), with the correlation coefficient r close to 1 (Fig. 3). According to Eq. (7), we can obtain β and c from the cases with different deformations for each aspect ratio (a/h). The Poisson's ratio for each case can be obtained by looking up Table 3 or Fig. 1 and applying linear interpolation.

In comparison with the actual value, the percentage errors of the calculated Poisson's ratio are between –1.7% to –8.2% when the aspect ratio is between 0.6 and 2 (Table 4). The percentage error of the Poisson's ratio is limited within –3.2% when the aspect ratio (a/h) is between 1 and 2. For the Young's modulus, the percentage errors of the calculated values are between +3.0% to +7.2% when the aspect ratio is between 1 and 2.

The error for the calculation of Young's modulus increased if the Poisson's ratio was assumed to be more different (v= 0.3, 0.35, 0.4 and 0.5) from its actual value (0.45) for the case of aspect ratio (a/h) = 1 (Table 5). As the percentage change of incorrectly assumed Poisson's ratios ranged from -33.3% to +11.1%, the corresponding percentage changes of the Young's moduli were from -19.1% to

+42.8%. The result indicated that if we incorrectly assumed the Poisson's ratio during the calculation, it would induce a large error in the estimation of Young's modulus.

4. DISCUSSION

In this paper, we reported a new method to determine the modulus and the Poisson's ratio simultaneously using a single indentation based on our finding that the scaling factor κ_n in Hayes' indentation solution [11] linearly depends on the deformation *w*. We extracted the relationship between the Poisson's ratio *v* and the deformation-dependent indentation stiffness using the previously published data [13]. Since the deformation-dependent indentation stiffness can also be obtained from the force-deformation data of an indentation test, the Poisson's ratio can then be calculated. Using the data of FE simulation for indentation, we have successfully demonstrated the feasibility of this new method. In the current study, the material was assumed linearly elastic, homogeneous, and isotropic.

The percentage errors of the estimated Poisson's ratio were within ±3.2% in comparison with the assigned values in FE simulation when the aspect ratio a/h ranged from 1 to 2. The corresponding percentage errors of the estimated Young's modulus ranged from +3.0% to +7.2%. The errors were rather stable when different deformations (1% to 10%) were used for the estimation. The robustness of the estimation could be further improved by averaging the parameters calculated using different deformation levels (last 4 rows in Table 4). This averaging approach could be particularly useful when the proposed method is applied for the real indentation data, as various noises may exist in the experimental force or deformation data. For the simulated cases with the aspect ratio (a/h) smaller than 1, the errors for the estimation of Poisson's ratio and Young's modulus were larger. For the cases that calculated in this study, the maximum estimation errors were -8.2% for the Poisson's ratio and 9.1% for the Young's modulus when the aspect ratio was 0.6 and the deformation was 10%. Since both the aspect ratio and the maximum deformation of an indentation can be controlled by the operator, the optimized indentation parameters can be used in real tests so as to reduce the estimation errors. The estimated errors observed in this study could be due to the computation errors in the FE simulation for indentation or the errors of κ reported in the previous study [13], which was also calculated using FE simulation. As demonstrated in Table 1, the maximum simulation error for the scaling factor is 3.3% under the condition of an infinitesimal deformation. This error is similar to the error of the Poisson's ratio estimation, which is 3.2% (a/h= 1 ~ 2). Therefore, to further improve the estimation accuracy, the scaling factor κ_n for different Poisson's ratio, aspect ratio, and deformation should be calculated more precisely using finite element or numerical analyses.

Our results also demonstrated that the estimation for the Young's modulus would be dramatically affected if the Poisson's ratio was incorrectly assumed. If the Poisson's ratio was assumed to be 0.3 and 0.5 rather than the real value of 0.45, the estimation error for the Young's modulus was -19.1% and 42.8% respectively when the aspect ratio was 1. The results confirmed the importance of the simultaneous measurement of Poisson's ratio when the indentation test is used to measure Young's modulus of the tissue.

It is interesting for us to understand, at least qualitatively, why the Poisson's ratio and Young modulus can be obtained from the force-deformation data of a single indentation, which only measures the force and deformation of the material in the axial direction. For a linearly elastic material, when it is compressed in one direction, it will expand in other two directions if the Poisson's ratio is not zero. This phenomenon has been used for the measurement of Poisson's ratios with a setup of unconfined condition [21]. During indentation, this lateral expansion is still there, but difficult to achieve as the material is continuous in the lateral directions. Instead, the material may bulge at locations surrounding the indentor. Balakrishnan and Socrate (2008) recently used secondary displacement sensors to monitor the bulging during indentation and found that this additional information could help to discern between materials with varying degrees of compressibility, i.e. different values of Poisson's ratio [33]. While the material surrounding the indentor bulges, additional force from this part of material would also be applied to the indentor, which requires a larger indentation force to maintain a certain indentation depth. If the Poisson's ratio of a material is 0, its indentation force-deformation will be only determined by the Young's modulus. Therefore, its indentation force will be linearly proportional to the applied deformation. If the Poisson's ratio is not 0, the shear force will contribute more through the lateral interaction to the overall indentation force as the increase of the deformation. This forms the nonlinearity of the indentation force-deformation curve, i.e. the deformation-dependent indentation stiffness (P/w) increases as the increase of deformation ratio (w/h). For different Poisson's ratios, the deformation-induced changes of the indentation stiffness are different. Therefore, we can calculate the Poisson's ratio from the deformation-dependent indentation stiffness if we can have an established table for their relationship. In this study, we established such a table for different aspect ratios (a/h) and a method to use this table for the calculation of the Poisson's ratio from indentation data.

The above elaboration is based on the assumption of a linearly elastic material, and the material stiffening observed during indentation tests come from the effect of non-zero Poisson's ratio under this condition. However, the material stiffening can also come from the nonlinearity of the material being tested. Earlier studies using spherical indentors have confirmed that applying the secondary displacement sensors to quantify the Poisson's ratio [33] and artificial neural networks to extract Poisson' ratio from indentation data [21] could be used for materials with both linear and nonlinear mechanical properties. In this study, we assumed that the material remains linear for all the indentation deformations (up to 10%). For real biological tissues, the nonlinearity of the material properties should also be considered [34,35]. Since the nonlinearity of the force-deformation data could be affected by both the material properties and the indentation, it would become more challenge to use the proposed technique. Further studies should be followed to investigate whether the method proposed in the current study can still be used for materials with nonlinear constitutive equations. Furthermore, the viscoelasticity of tissues under indentation tests has been previously analyzed using quasilinear viscoelastic model (QLV) [35,36], where the Poisson's ratio was assumed. Further investigations are necessary to include this new method into QLV indentation analysis so as to extract Poisson's ratio simultaneously with other QLV parameters. In the real situation, particularly in the case of biological tissues, the substrate underlying the tissue may not be to totally flat [37]. Therefore the sensitivity of the estimation of Poisson's ratio on the curvature of the tissue substrate using the proposed method needs to be further studied as well. It should also be investigated in future studies how the inhomogeneity and anisotropy of tissues affect the performance of the method introduced in this study.

5. CONCLUSIONS

The results from the FE simulation showed that the proposed method is feasible to determine the Young's modulus and Poisson's ratio simultaneously using the force-deformation data obtained from a single cylindrical indentation in a linearly elastic, homogeneous, isotropic material. . According to the results of this study, the optimized aspect ratio for indentation is between 1 and 2. Therefore, the new method may be particularly useful to determine the parameters needed to characterize tissues which are thin enough such as articular cartilage. We can use a larger indentor when the tissue is relatively thick in order to keep the aspect ratio larger than 1. The use of a simple table searching method in the calculation of Poisson's ratio make it much faster in comparison with previous methods using artificial neural networks or genetic algorithms [30,32]. Further experiments on tissue phantoms and biological tissues *in-vitro* and *in-vivo* will be performed to demonstrate the feasibility of this new method for the real indentation data.

ACKNOWLEDGEMENTS

This work was partially supported by the Research Grants Council of Hong Kong (PolyU 5245/03E, PolyU5318/05E) and The Hong Kong Polytechnic University (J-BB69).

REFERENCES

1. Hasler E M, Herzog W, Wu J Z, Muller W and Wyss U 1999 Articular cartilage biomechanics: Theoretical models, material properties, and biosynthetic response *Crit. Rev. Biomed. Eng.* **27** 415-488

2. Gouldstone A, Chollacoop N, Dao M, Li J, Minor A M and Shen Y L 2007. Indentation across size scales and disciplines: Recent developments in experimentation and modeling *Acta Mater.* **55** 4015-4039.

3. Athanasiou K A, Rosenwasser M P, Buckwalter J A, Malinin T I and Mow V C 1991 Interspecies comparisons of insitu intrinsic mechanical properties of distal femoral cartilage *J. Orthop. Res.* **9** 330-340

4. Athanasiou K A, Agarwal A and Dzida F J 1994 Comparative study of the intrinsic mechanical properties of the human acetabular and femoral head cartilage *J. Orthop.* R*es.* **12** 340-349

5. Hori R Y and Mockros L F 1976 Indentation tests of human articular cartilage *J. Biomech.* **9** 259-268

6. Mak A F, Lai W M and Mow V C 1987 Biphasic indentation of articular cartilage - I. Theoretical analysis *J. Biomech.* **20** 703-714

7. Mow V C, Gibbs M C, Lai W M, Zhu W B and Athanasiou K A 1989 Biphasic Indentation of articular cartilage – II. A numerical algorithm and an experimental study *J. Biomech.* **22** 853-861

8. Lyyra T, Jurvelin J, Pitkanen P, Vaatainen U and Kiviranta I 1995 Indentation instrument for the measurement of cartilage stiffness under arthroscopic control *Med. Eng. Phys.* **17** 395-399

9. Suh J K F, Youn I and Fu F H 2001 An in situ calibration of an ultrasound transducer: a potential application for an ultrasonic indentation test of articular cartilage *J. Biomech.* **34** 1347-1353

10. Toyras J, Lyyra L T, Niinimaki M, Lindgren R, Nieminen M T, Kiviranta I and Jurvelin J S 2001 Estimation of the Young's modulus of articular cartilage using

an arthroscopic indentation instrument and ultrasonic and ultrasonic measurement of tissue thickness *J. Biomech.* **34** 251-256

11. Hayes W C, Herrmann G, Mockros L F and Keer L M 1972 Mathematical analysis for indentation tests of articular cartilage *J. Biomech.* **5** 541-551
12. Jurvelin J S 1991 Biomechanical properties of the knee articular cartilage under various loading conditions, *PhD thesis*, University of Kuopio, Kuopio, Finland.
13. Zhang M, Zheng Y P and Mak A F T 1997 Estimating the effective Young's modulus of soft tissues from indentation tests – nonlinear finite element analysis of effects of friction and large deformation *Med. Eng. Phys.* **19** 512-517
14. Swann A C and Seedhom B B 1989 Improved techniques for measuring the indentation and thickness of articular cartilage *Proc. Inst. Mech. Eng .[H]* **203** 143-150
15. Jurvelin J S, Rasanen T, Kolmonen P and Lyyra T 1995 Comparison of optical, needle probe and ultrasonic techniques for the measurement of articular cartilage thickness *J. Biomech.* **28** 231-235
16. Zheng Y P and Mak A F T 1996 An ultrasound indentation system for biomechanical properties assessment of soft tissue *in-vivo IEEE Trans. Biomed. Eng.* **43** 912-918
17. Fleming B C and Beynnon B D 2004 *In Vivo* Measurement of Ligament/ Tendon Strains and Forces: A Review *Ann. Biomed. Eng.* **32** 318-328
18. Barker M K and Seedhom B B 1997 Articular cartilage deformation under physiological cyclic loading – apparatus and measurement technique *J. Biomech.* **30** 377-381

19. Klaesner J W, Commean P K, Hastings M K, Zou D Q and Mueller M J 2001 Accuracy and reliability testing of a portable soft tissue indentor *IEEE Trans. Neural Syst. Rehabil. Eng.* **9** 232-240

20. Laasanen M S, Toyras J, Hirvonen J, Saarakkala S, Korhonen R K, Nieminen M T, Kiviranta I. and Jurvelin J S 2002 Novel mechano-acoustic technique and instrumentation for diagnosis of cartilage degeneration *Physiol. Meas.* **23** 491-503

21. Jurvelin J S, Buschmann M D and Hunziker E B 1997 Optical and mechanical determination of Poisson's ratio of adult bovine humeral articular cartilage *J. Biomech.* **30** 235-241

22. Konofagou E and Ophir J 1998 A new elastographic method for estimation and imaging of lateral displacements, lateral strains, corrected axial strains and Poisson's ratios in tissues *Ultras. Med. Biol.* **24** 1183-1199.

23. Fortin M, Buschmann M D, Bertrand M H, Foster F S and Ophir J 2003 Dynamic measurement of internal solid displacement in articular cartilage using ultrasound backscatter *J. Biomech.* **36** 443-447

24. Righetti R, Ophir J, Srinivasan S and Krouskop T A 2004 The feasibility of using elastography for imaging the Poisson's ratio in porous media *Ultras. Med. Biol.* **30** 215-228

25. Simi C 2006 Reconstructions of shear modulus, Poisson's ratio, and density using approximate mean normal stress lambda epsilon(alpha alpha) as unknown *IEEE Trans Ultras. Ferroelectr. Freq. Contr.* **53** 2416-2434

26. Jin H and Lewis J L 2004 Determination of Poisson's ratio of articular cartilage by indentation using different sized indenters *J. Biomech. Eng.* **126** 138-145

27. Choi A P C and Zheng Y P 2005 Estimation of Young's modulus and Poisson's ratio of soft tissue from indentation using two different-sized indentors: finite

element analysis of the finite deformation effect *Med. Biol. Eng. Comput.* **43** 258-264

28. Lucas B N, Hay J C and Oliver W C 2004 Using multidimensional contact mechanics experiments to measure Poisson's ratio *J. Mater. Res.* **19** 58-65

29. Jennet N M, Aldrich-Smith G and Maxwell A S 2004 Validated measurement of Young's modulus, Poisson ratio, and thickness for thin coatings by combing instrumented nanoindentation and acoustical measurement *J. Mater. Res.* **19** 143-148

30. Huber N, Konstantinidis A and Tsakmakis Ch 2001 Determination of Poisson's ratio by spherical indentation using neural networks – Part II: Identification method *Trans. ASME J. Appl. Mech.* **68** 224-229

31. Huber N and Tsakmakis Ch 2001 Determination of Poisson's ratio by spherical indentation using neural networks – Part I: Theory *Trans. ASME J. Appl. Mech.* **68** 218-223

32. Ling H Y, Choi P C, Zheng Y P and Lau K T 2007 Extracting the mechanical properties of soft tissues using ultrasound indentation associated with genetic algorithm. *J. Mater. Sci.: Mater. Med.* **18** 1579-1586

33. Balakrishnan A and Socrate S 2008 Material property differentiation in indentation testing using secondary sensors *Experim. Mech.* **48** 549-558.

Liu Y, Kerdok A E and Howe R D 2004 A Nonlinear finite element model of soft tissue indentation *Lect. Notes Comp. Sci.* **3078** 67-76

34. Zheng Y P and Mak A F T 1999 Extraction of quasilinear viscoelastic parameters for lower limb soft tissues from manual indentation experiment *J. Biomech. Eng.* **121** 330-339

35. Huang Y P, Zheng Y P, and Leung S F 2005 Quasilinear viscoelastic parameters of neck tissues with fibrosis induced by radiotherapy *Clin. Biomech.* **20** 145-154

36. Lu MH and Zheng YP 2004 Indentation test of soft tissues with curved substrates: a finite element study *Med. Biol. Eng. Comp.* **42** 535-540.

Table 1. Comparison of the scaling factor (κ) values obtained by the FE model used in the current study, which was established based on that reported by Zhang et al. (1997), and the numerical analyses (Hayes et al., 1972; Jurvelin 1991) for the case of an infinitesimal indentation depth (0.1%).

	Poisson's ratio																				
	0.10			0.20			0.30			0.35			0.40			0.45			0.50		
a/h	Jurvelin	Present	% error	Jurvelin	Present	% error	Hayes	Present	% error	Hayes	Present	% error	Hayes	Present	% error	Hayes	Present	% error	Hayes	Present	% error
0.2	1.183	1.207	2.04	1.192	1.212	1.69	1.207	1.218	0.94	1.218	1.221	0.28	1.232	1.228	-0.35	1.252	1.233	-1.50	1.281	1.242	-3.06
0.4	1.413	1.459	3.26	1.434	1.479	3.14	1.472	1.513	2.81	1.502	1.540	2.54	1.542	1.577	2.27	1.599	1.624	1.54	1.683	1.695	0.69
0.6	1.677	1.717	2.39	1.715	1.755	2.33	1.784	1.821	2.06	1.839	1.871	1.72	1.917	1.939	1.15	2.031	2.033	0.08	2.211	2.177	-1.53
0.8	1.963	1.997	1.72	2.018	2.055	1.84	2.124	2.154	1.43	2.211	2.231	0.91	2.338	2.340	0.08	2.532	2.495	-1.47	2.855	2.785	-2.44
1.0	2.260	2.294	1.48	2.334	2.371	1.60	2.480	2.523	1.75	2.603	2.620	0.63	2.789	2.778	-0.39	3.085	3.060	-0.82	3.609	3.583	-0.73
1.5	3.030	3.104	2.44	3.149	3.219	2.24	3.400	3.476	2.22	3.629	3.708	2.17	3.996	4.076	1.99	4.638	4.725	1.88	5.970	6.039	1.16
2.0	3.804	3.895	2.38	3.966	4.055	2.24	4.336	4.425	2.05	4.685	4.777	1.96	5.272	5.360	1.68	6.380	6.464	1.32	9.070	9.046	-0.26

Table 2. The scaling factor (κ) used in this study for different aspect ratios (a/h), Poisson's ratios (v) and deformation ratios (w/h).

a/h = 2	Poisson's ratio						
w/h	0.10	0.20	0.30	0.35	0.40	0.45	0.50
0.001	3.895	4.055	4.424	4.777	5.360	6.464	9.046
0.01	3.906	4.068	4.446	4.805	5.405	6.550	9.308
0.025	3.922	4.089	4.476	4.848	5.473	6.679	9.070
0.05	3.950	4.123	4.528	4.919	5.585	6.893	10.357
0.1	4.006	4.192	4.631	5.061	5.809	7.322	11.667
a/h = 1.5							
0.001	3.104	3.219	3.476	3.708	4.076	4.725	6.039
0.01	3.111	3.229	3.490	3.728	4.109	4.781	6.193
0.025	3.121	3.242	3.512	3.759	4.158	4.875	6.424
0.05	3.138	3.265	3.549	3.811	4.241	5.025	6.809
0.1	3.173	3.311	3.622	3.915	4.406	5.326	7.579
a/h = 1							
0.001	2.294	2.371	2.523	2.620	2.778	3.060	3.583
0.01	2.294	2.374	2.530	2.632	2.798	3.090	3.636
0.025	2.294	2.377	2.541	2.651	2.829	3.136	3.715
0.05	2.294	2.383	2.558	2.682	2.879	3.213	3.847
0.1	2.295	2.394	2.592	2.745	2.980	3.366	4.112
a/h = 0.8							
0.001	1.997	2.055	2.154	2.231	2.340	2.495	2.785
0.01	1.997	2.056	2.159	2.239	2.354	2.520	2.828
0.025	1.997	2.057	2.166	2.252	2.375	2.558	2.893
0.05	1.998	2.059	2.177	2.273	2.410	2.621	3.001
0.1	2.000	2.062	2.199	2.314	2.479	2.747	3.217
a/h = 0.6							
0.001	1.717	1.755	1.821	1.871	1.939	2.033	2.177
0.01	1.717	1.755	1.822	1.875	1.947	2.048	2.205
0.025	1.718	1.756	1.824	1.881	1.958	2.070	2.248
0.05	1.718	1.757	1.827	1.891	1.978	2.108	2.318
0.1	1.719	1.759	1.834	1.911	2.017	2.183	2.459
a/h = 0.4							
0.001	1.459	1.479	1.513	1.540	1.577	1.624	1.695
0.01	1.459	1.479	1.514	1.542	1.581	1.632	1.710
0.025	1.460	1.480	1.515	1.546	1.587	1.645	1.734
0.05	1.460	1.480	1.516	1.551	1.598	1.666	1.773
0.1	1.461	1.481	1.519	1.562	1.619	1.708	1.850
a/h = 0.2							
0.001	1.207	1.212	1.218	1.221	1.228	1.233	1.242
0.01	1.207	1.212	1.219	1.224	1.231	1.240	1.254
0.025	1.207	1.212	1.219	1.227	1.237	1.250	1.271
0.05	1.208	1.213	1.221	1.232	1.246	1.267	1.301
0.1	1.209	1.214	1.223	1.243	1.265	1.302	1.359

Table 3. The relationship between the factor β, Poisson's ratio (v), and aspect ratio (a/h).

	aspect ratio a/h						
v	0.2	0.4	0.6	0.8	1	1.5	2
0.10	0.012	0.014	0.012	0.016	0.004	0.222	0.286
0.20	0.012	0.014	0.023	0.034	0.098	0.284	0.338
0.30	0.035	0.037	0.073	0.208	0.271	0.421	0.466
0.35	0.179	0.141	0.215	0.373	0.478	0.559	0.595
0.40	0.301	0.265	0.401	0.597	0.728	0.810	0.838
0.45	0.554	0.519	0.740	1.012	1.002	1.271	1.327
0.50	0.946	0.920	1.295	1.551	1.478	2.550	2.897

Table 4. The Poisson's ratio and Young's modulus extracted from the simulated indentation data using the new approach for the cases with different aspect ratios (from 0.6 to 2) and deformations (from 1% to 10%). The percentage errors indicate the difference between the estimated and real values of the parameters. The Young's modulus and Poisson's ratio assigned for the FE simulations were 60 kPa and 0.45, respectively.

w/h	Parameters	aspect ratio *a/h*					mean	% error
		0.6	0.8	1.0	1.5	2		
0.1	*v*	0.413	0.420	0.438	0.438	0.440	0.430	-4.5 %
	% error	-8.2 %	-6.7 %	-2.6 %	-2.8 %	-2.2 %		
	E	65.4	65.3	62.6	63. 7	63.7	64.1	6. 9 %
	% error	9.1%	8.9%	4.3 %	6.1 %	6.1 %		
0.05	*v*	0.423	0.423	0.440	0.436	0.439	0.432	-4.00 %
	% error	-5.9 %	-6.0 %	-2.3 %	-3.0 %	-2.5 %		
	E	63.9	64.7	62.3	64.0	64.1	63.8	6.34 %
	% error	6.5 %	7.9 %	3.8 %	6.6 %	6.9 %		
0.025	*v*	0.429	0.425	0.441	0.436	0.438	0.435	-3.2 %
	% error	-4.8 %	-5.5 %	-2.1 %	-3.2 %	-2.7 %		
	E	63.128	64.306	62.078	64.180	64.340	63.6	6.0 %
	% error	5.2 %	7.2 %	3.5 %	7.0 %	7.2 %		
0.01	*v*	0.424	0.426	0.442	0.436	0.438	0.433	-3.7 %
	% error	-5.8 %	-5.4 %	-1.7 %	-3.1 %	-2.6 %		
	E	63.8	64.3	61.8	64.1	64.2	63.6	6.0 %
	% error	6.3 %	7.1 %	3.0 %	6.8 %	7.1 %		
	v mean	0.422	0.424	0.440	0.437	0.439		
	v % error	-6.2 %	-5. 9 %	-2.2 %	-3.0 %	-2.5 %		
	E mean	64.1	64.7	62.2	64.0	64.1		
	E % error	6.8 %	7.8 %	3.7 %	6.6 %	6.8 %		

Table 5. The Young's moduli estimated using different assumed Poisson's ratio (0.3, 0.35, 0.4 and 0.5). The assigned parameters for the FE simulation are (*E*) = 60kPa, (*v*) = 0.45, and (*a/h*)=1. The values in the bracket indicate the percentage differences between the estimated and real moduli.

Assumed Poisson's ratio (*v*) (Percentage change)	Percentage deformation			
	1 %	2.5 %	5 %	10 %
0.30 (-33.3 %)	85.7 (+42.8 %)	85.7 (+42.8 %)	85.7 (+42.8 %)	85.7 (+42.8 %)
0.35 (-22.2 %)	78.7 (+31.2 %)	78.7 (+31.2 %)	78.7 (+31.2 %)	78.7 (+31.2 %)
0.40 (-11.1 %)	70.3 (+17.2 %)	70.3 (+17.2 %)	70.3 (+17.2 %)	70.3 (+17.2 %)
0.50 (11.1 %)	48.5 (-19.1 %)	48.5 (-19.1 %)	48.5 (-19.1 %)	48.5 (-19.1 %)

Figure Captions

Figure 1. The relationship between factor β and Poisson's ratio (v) for different aspect ratio (a/h). From these curves, factor β can be used to determine the Poisson's ratio by interpolation. For instance, when (β) = 1.25 and (a/h) = 2, the estimated (v) = 0.44 (the real Poisson's ratio was 0.45 for this case).

Figure 2. A typical set of force-deformation data obtained using the FE simulation for indentation with (a/h) = 2, (E) = 60kPa, and (v) = 0.45. The force-deformation relationship is slightly nonlinear and it can be fitted by a quadratic function.

Figure 3. The relationship between the deformation dependent indentation stiffness (P/w) and deformation ratio (w/h) extracted from the indentation data shown in Figure 2. The assigned parameters for the FE simulation were (a/h) = 2, (E) = 60kPa, and (v) = 0.45. Linear regressions were performed for the data with different deformation ratios (w/h). We used the case with 10% deformation as an example, and the y-intercepts (c) and the slope ($c\beta$) were 4.38 and 5.46 respectively, so the obtained factor β was 1.25, which was used as an example to estimate the Poisson's in Figure 1.

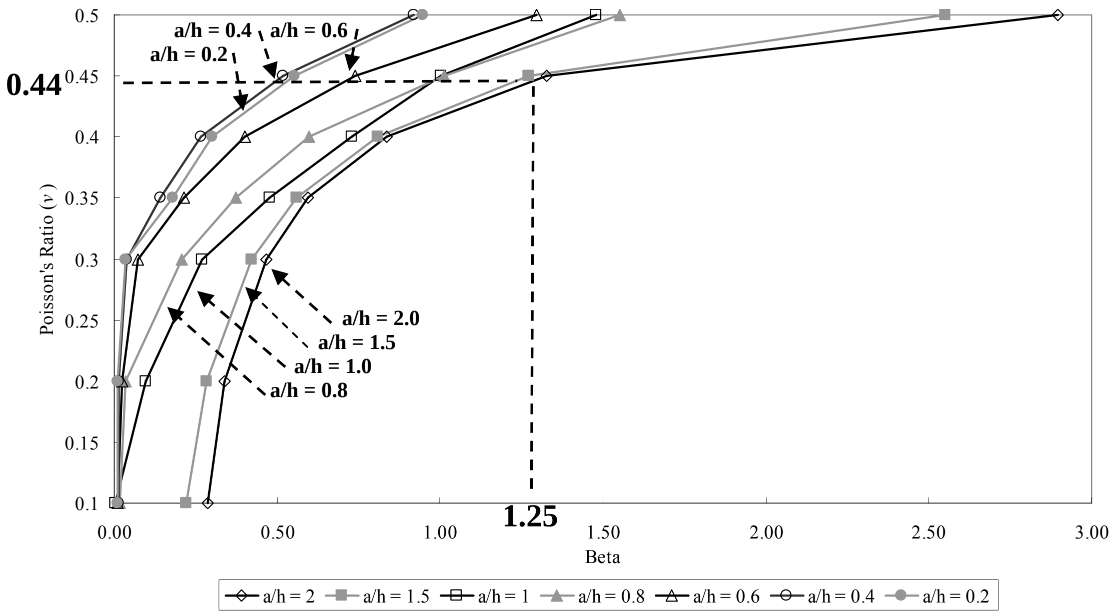

0.44
1.25
a/h = 0.4
a/h = 0.6
a/h = 0.2
a/h = 2.0
a/h = 1.5
a/h = 1.0
a/h = 0.8
Poisson's Ratio (v)
Beta
0.1
0.15
0.2
0.25
0.3
0.35
0.4
0.45
0.5
0.00
0.50
1.00
1.50
2.00
2.50
3.00
a/h = 2
a/h = 1.5
a/h = 1
a/h = 0.8
a/h = 0.6
a/h = 0.4
a/h = 0.2

Figure 1

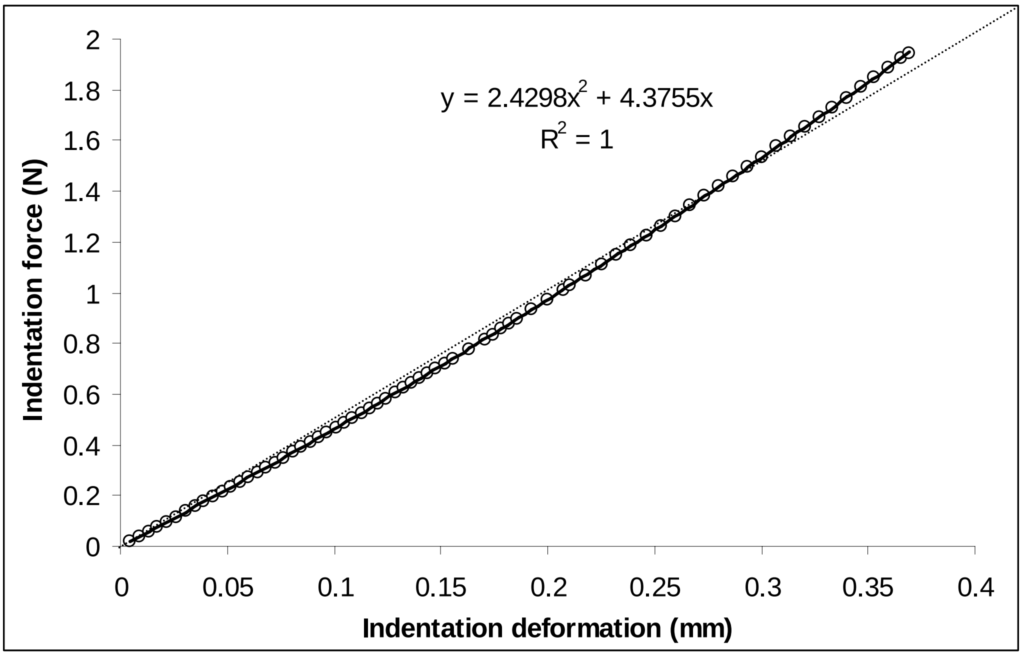
y = 2.4298x2 + 4.3755x
R2 = 1
Indentation force (N)
Indentation deformation (mm)
0
0.2
0.4
0.6
0.8
1
1.2
1.4
1.6
1.8
2
0
0.05
0.1
0.15
0.2
0.25
0.3
0.35
0.4

Figure 2

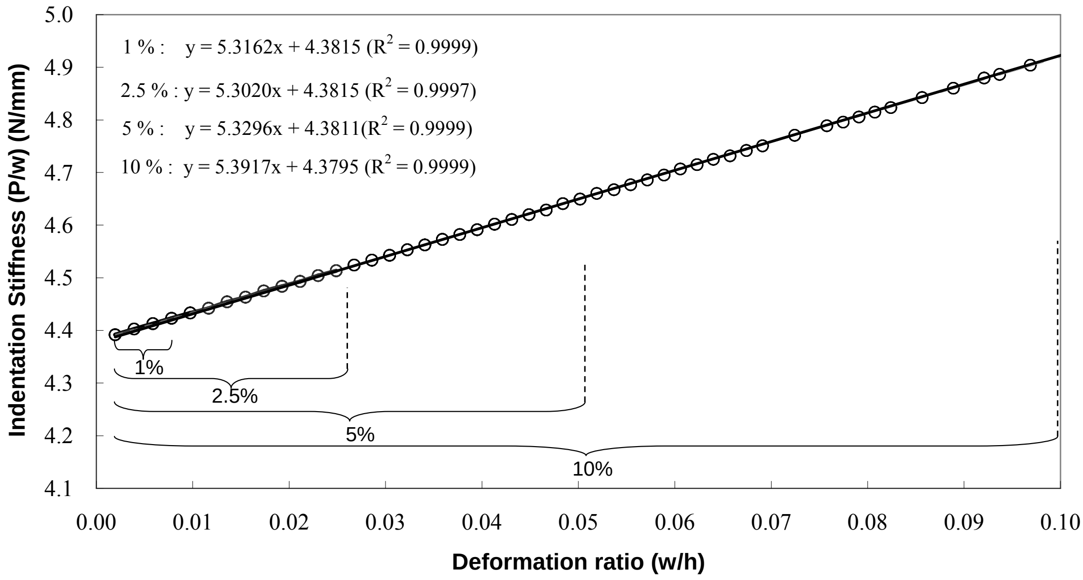
1 % : y = 5.3162x + 4.3815 (R2 = 0.9999)
2.5 % : y = 5.3020x + 4.3815 (R2 = 0.9997)
5 % : y = 5.3296x + 4.3811(R2 = 0.9999)
10 % : y = 5.3917x + 4.3795 (R2 = 0.9999)
1%
2.5%
5%
10%
Indentation Stiffness (P/w) (N/mm)
Deformation ratio (w/h)
5.0
4.9
4.8
4.7
4.6
4.5
4.4
4.3
4.2
4.1
0.00
0.01
0.02
0.03
0.04
0.05
0.06
0.07
0.08
0.09
0.10

Figure 3